Structural analysis of neomycin B and kanamycin A binding Aminoglycosides Modifying Enzymes (AME) and bacterial ribosomal RNA

Julia Revillo Imbernon, Jean-Marc Weibel, Eric Ennifar, Gilles Prévost, Esther Kellenberger

Received: 9 December 2023 | Revised: 6 March 2024 | Accepted: 13 March 2024

DOI: 10.1002/minf.202300339

RESEARCH ARTICLE

molecular informatics

Structural analysis of neomycin B and kanamycin A binding Aminoglycosides Modifying Enzymes (AME) and bacterial ribosomal RNA

Julia Revillo Imbernon[1] | **Jean-Marc Weibel**[2] | **Eric Ennifar**[3] | **Gilles Prévost**[4] | **Esther Kellenberger**[1]

[1]Laboratoire d'Innovation Thérapeutique, UMR7200 CNRS Université de Strasbourg, Faculté de Pharmacie, Illkirch-Graffenstaden, France

[2]Laboratoire de Synthèse, Réactivité Organiques et Catalyse, Institut de Chimie, UMR 7177 CNRS, Université de Strasbourg, Strasbourg, France

[3]Architecture et Réactivité de l'ARN, CNRS UPR 9002, Institut de Biologie Moléculaire et Cellulaire, Université de Strasbourg, Strasbourg, France

[4]Virulence bactérienne précoce: fonctions cellulaires et contrôle de l'infection aiguë et subaiguë, UR 7290 Université de Strasbourg, FMTS, ITI InnoVec, Strasbourg, France

Correspondence
Esther Kellenberger, Laboratoire d'Innovation Thérapeutique, UMR7200 CNRS Université de Strasbourg, Faculté de Pharmacie, 74 route du Rhin, 67400 Illkirch-Graffenstaden, France.
Email: ekellen@unistra.fr

Funding information
High-Performance Computing Center of the French National Institute for Nuclear and Particle Physics, Grant/Award Number: IN2P3; Centre National de la Recherche Scientifique (CNRS); Université de Strasbourg, Grant/Award Number: IDEX consolidation W19RHUS3; IdEx Unistra, Grant/Award Number: ANR-10-IDEX-0002; SFRI-STRAT'US project, Grant/Award Number: ANR-20-SFRI-0012

Abstract

Aminoglycosides are crucial antibiotics facing challenges from bacterial resistance. This study addresses the importance of aminoglycoside modifying enzymes in the context of escalating resistance. Drawing upon over two decades of structural data in the Protein Data Bank, we focused on two key antibiotics, neomycin B and kanamycin A, to explore how the aminoglycoside structure is exploited by this family of enzymes. A systematic comparison across diverse enzymes and the RNA A-site target identified common characteristics in the recognition mode, while assessing the adaptability of neomycin B and kanamycin A in various environments.

KEYWORDS
aminoglycoside N-Acetyltransferase, aminoglycoside O-Nucleotidyltransferase, aminoglycoside O-Phosphotransferase, binding mode, interactions

1 | INTRODUCTION

Since the discovery of streptomycin in 1943, aminoglycoside antibiotics (AGAs) have been crucial in the treatment of various Gram-positive and Gram-negative bacterial infections. AGAs derive from substances produced by the species *Streptomyces* or *Micromonospora* and are effective against a wide range of bacterial pathogens, including the members of the Enterobacteriaceae family, many *Mycobacterium* spp., *S. aureus*, *Listeria*, non mucoid *P. aeruginosa*, and *A. baumannii* in a lesser extent [1,2]. This therapeutical class enters bacteria through the membranous respiratory apparatus and binds the bacterial small 30S subunit on 16S ribosomal RNA subunit at the tRNA acceptor site A. The binding leads to the misread of mRNA, and thus to the synthesis of non-functional proteins which can ultimately cause the death of the bacterial cell [3,4]. Aminoglycosides have shown their interest in the treatment of genetic diseases, thanks to their ability to suppress premature termination codons (PTCs). They were also studied for the treatment of HIV as they can target many *in vitro* steps of the virus life cycle [5].

Gentamicin, amikacin, and tobramycin are the most clinically used aminoglycosides because of their reliable activity against Gram-negative aerobic *bacilli* [1,6]. Generally, AGAs cannot be absorbed by the intestine tract and are hence administered via topical, inhalation, or parenteral routes. Neomycin and paromomycin are the exceptions to this rule as their low absorption make them useful to suppress the intestinal bacterial flora [1]. Nevertheless, the prolonged use of these antibiotics can cause nephrotoxicity or ototoxicity. Indeed, the excretion of aminoglycosides is mainly operated by the kidneys. The partial reabsorption of AGAs during the nephron reabsorption step causes the death of kidney epithelial cells. However, this renal toxicity is generally reversible thanks to the regeneration capacity of proximal tubular cells [7]. On another side, the ototoxicity occurs in patients carrying a punctual mutation of the mitochondrial 12S rRNA on the internal ear cells. The mutation A1555G or C1494U renders the sequence of the mitochondrial 12S rRNA similar to the bacterial rRNA aminoglycosides target on bacteria and thus, binds the AGAs irreversibly [8]. Despite toxicity, aminoglycosides are listed as essential medicines by the WHO and are still crucial against the Gram-negative bacterial infections [9,10].

After 80 years on the market, another limitation tackles aminoglycosides. Different AGAs resistance mechanisms were selected and have emerged such as the modification of the active site due to ribosome mutations [11], methylations by 16S rRNA methyltransferases [12], drug efflux [13] or the decrease of bacteria membrane permeability [14]. However, the most common mechanism of resistance is assigned to Aminoglycoside-Modifying Enzymes [15].

Aminoglycoside-Modifying Enzymes (AMEs) are an effective resistance mechanism able to metabolize all existing aminoglycosides. In 2010, a staggering number of 120 different AMEs were reported, highlighting the diversity and complexity of these enzymes [15]. More simply, AMEs can be classified by catalytic activity resulting in only 3 types: Aminoglycoside N-Acetyltransferase (AAC), Aminoglycoside O-Phosphotransferase (APH) and Aminoglycoside O-Nucleotidyltransferase (ANT) (Figure 1A). To accomplish their biological activity, each AME requires a cofactor, and a divalent ion in the case of APHs and ANTs. Each AME has a specific resistance profile and metabolizes one position of the targeted aminoglycosides. Thus, aminoglycosides are targeted by a large but specific enzymatic modification profile. Specific examples for neomycin B and kanamycin A are shown in Figure 1B [15].

Many efforts have been made since the early 1970s to develop aminoglycoside derivatives that are highly effective, minimally toxic, and capable of overcoming bacterial resistance [16–18]. Significant advancements in chemistry have led to the production of a broad range of amino-modified glycosides, culminating in the introduction of novel drugs in the 2010's, called plazomicin [19]. Regrettably, bacteria have rapidly developed resistance to all semi-synthetic aminoglycosides, including plazomicin, highlighting the critical need for ongoing research and development of alternative treatments [15,20].

In addition to investigating the relationship between structure and activity, the analysis of the three-dimensional structures of aminoglycosides has served as the foundation for comprehending their antibiotic activity. The mechanism of action of aminoglycosides was uncovered in 1965 [3], but it took 20 years to identify the binding site of these compounds [4,21]. The first image of the 30S ribosomal particle bound to an aminoglycoside was obtained through X-ray crystallography in 2000 [22]. With the advent of the genomic era and

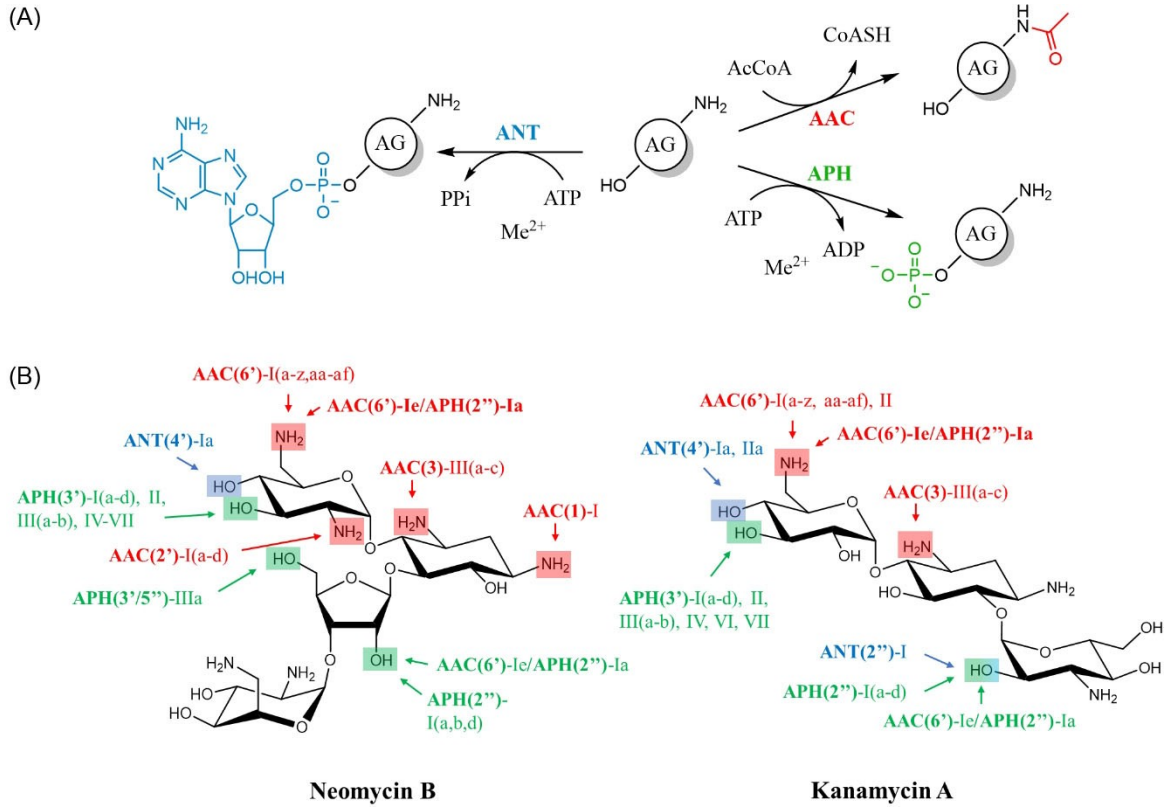

FIGURE 1 Mechanism of action of AMEs on aminoglycosides. (A) Reactions catalyzed by the three type of AMEs. Where AAC or acetyltransferase transfers an acetyl group to a free amino group, APH or phosphotransferase transfers a phosphate group to a free hydroxyl, and ANT or nucleotidyltransferase transfers a nucleotide to a free hydroxyl. The cofactors used by the enzymes are specified on the reaction path. The transferred groups are depicted in color. Image adapted from article 15. (B) Enzymatic modification profile of neomycin B and kanamycin A. The Arabic number between brackets corresponds to the modified position on the AGA. The Roman number relates to the resistance profile.

advancements in technology, the discovery and design of antibiotics have shifted towards target-based strategies [23]. Consequently, since the 2000s, there has been a growing number of crystallographic structures published. Initially, research focused on investigating the mechanism of action of aminoglycosides by crystallizing the 30S ribosomal subunits in complex with tRNA, mRNA, and AGAs [24]. Subsequently, studies of AGAs-RNA complexes that did not include the ribosomal subunit gained popularity between 2015 and 2019. Finally, the need to overcome resistance has led to an increased focus on AGAs-AMEs complexes, with 35 of the 82 existing structures published between 2015 and 2019, and 22 since the beginning of 2020 [24]. In brief, research on the AGAs primary target has shed light on the molecular mechanisms underlying antibiotic action, while studies on AMEs have revealed how these enzymes can metabolize one or more substrates in the aminoglycoside family. However, only a limited number of studies have investigated the interplay between different types of target biomolecules and AGAs. In a comprehensive structural study carried out in 2003, Vicens and Westhof showed that neamine, which is composed of rings I and II and is conserved in almost all AGAs, plays a critical role in binding to the ribosomal site A and AMEs [21]. Both binding sites have negatively charged residues on their surface, which are complementary to the positively charged amine groups in AGAs, and thus, the binding modes are dominated by electrostatic interactions and hydrogen bonds. This study was however based on a limited number of structures: 14 PDB entries, including five complexes between an AGA and the 30S subunit, three complexes between an AGA and synthetic RNA fragments containing two A-sites, and six complexes with three different AMEs.

In this review, we provide an inventory of the structures of AMEs available in the Protein Data Bank (PDB), with a focus on the recognition mode of two leading AGAs, namely neomycin B and kanamycin A. Neomycin B and kanamycin A belong to 4,5-2-DOS disubstituted and 4,6-2-DOS disubstituted AGAs, respectively, and are among the most documented aminoglycosides in their class in the PDB. The structures of these two AGAs indeed cover the three types of AMEs, but also the RNA A-

site target. We have conducted a systematic comparison of the binding modes of these two AGAs to their respective binding sites and we will here present the conclusions derived from this analysis. Firstly, we will outline the chemical groups that form non-covalent bonds with different types of AMEs with the aim of identifying common or specific recognition positions for these enzymes. Secondly, we will describe the conformations of neomycin B and kanamycin A in their bound forms to evaluate the adaptability of these two AGAs to the protein environments of AMEs. Finally, we will revisit our findings in light of the requirements needed for RNA binding and the functionalizations prone to prevent AME binding.

2 | MATERIALS AND METHODS

2.1 | Collection of AME-AGA complexes from PDB

Three dimensional structures of AMEs containing neomycin B or kanamycin A (HET codes: NMY or KAN, respectively) were selected from the PDB website and saved under mmCIF format. The published sc-PDB protocol [25,26] was followed for the preparation, standardization, and binding site detection of the complexes. In this protocol, the all-atom description of molecules, including hydrogen, was prepared using Protoss (v4.0, ZBH, University of Hamburg, Germany) [27]. Entries failing at any step of the protocol were discarded. Covalently linked aminoglycosides were ignored. The aminoglycoside binding site in the AME was defined as all the residues at a maximum distance of 6.5 Å from the aminoglycoside. For each of the AME-AGA structures, the aminoglycoside, the protein, and its binding site were recorded in three separate files in MOL2 format. Water molecules were included in the protein and the site provided forming at least two hydrogen bonds with the protein and one with the aminoglycoside. Metal cations were also included in the protein and the site. This is not the case for the other cofactors, discarded because of their inconsistent description.

2.2 | Collection of RNA-AGA complexes from PDB

Three dimensional structures of the bacterial A site containing neomycin B and kanamycin A were downloaded from the PDB website. The residues constituting the bacterial ribosomal site A and having at least one atom at a distance of 6.5 Å from the aminoglycoside were extracted from the PDB structure and saved under PDB format using MOE (2022.02 Chemical Computing Group ULC, 1010 Sherbooke St. West, Suite #910, Montreal, QC, Canada, H3 A 2R7). The protonation was performed using Protoss (v4.0, ZBH, University of Hamburg, Germany) [27]. The correct valences of all atoms were verified by using RDKit tools (RDKit: Open-source cheminformatics, https://www.rdkit.org, https://doi.org/10.5281/zenodo.7415128). Water molecules forming at least two hydrogen bonds with the RNA and one with the aminoglycoside were included in the complex.

2.3 | Assessment of the quality of structures

Entries with resolution higher than 3.5 Å were discarded. The quality of structures was evaluated using Real-Space Correlation Coefficient (RSCC) following the Twilight classification: RSCC >0.9 states that the model fits the electron density, $0.9>\text{RSCC}>0.8$ is given to a model partially fitting the electron density, $\text{RSCC}<0.8$ advertises about models with questionable quality to be used with caution. The RSCC of the ligands was extracted from the "validation XML" file present on the PDB website for each entry. The mean RSCC of the binding site residues was calculated by using the score given for each amino acid on the "validation XML" file.

2.4 | Interactions analysis

The interactions formed between the aminoglycoside and the AME binding site were detected using IChem (v5.2.8, University of Strasbourg, France) [28,29]. IChem relies on geometric rules to identify ionic bonds, hydrogen bonds, metallic interactions, aromatic stacking, and hydrophobic contacts. IChem generates a MOL2 file containing three pseudoatoms per interaction: one representing the ligand atom(s) which is (are) involved in the interaction; one representing the protein atom(s) which is (are) involved in the interaction; and one at the center of the segment defined by these two points.

The interactions formed between the aminoglycoside and the RNA were detected by calculating the distances (3.5 Å for hydrogen bonds and 4 Å for ionic bonds) and angles ($>120°$) between the atoms with RDKit (RDKit: Open-source cheminformatics, https://www.rdkit.org, https://doi.org/10.5281/zenodo.7415128).

2.5 | Aminoglycoside conformational analysis

The root mean square deviation (RMSD) of the coordinates of neomycin B or kanamycin A was calculated using the pair-fit tool offered by PyMOL (v2.3.5, Schrodinger, LLC) through an all-against-all fit of all non-hydrogen atoms. The number of conformations was determined via a density-based clustering using Sklelarn (eps = 0.5) [30].

For display purposes, the 3D structures of an aminoglycoside were aligned based on rings I and II only (all non-hydrogen atoms except C(6')-NH_2).

The dihedral angles of the linkage between the rings of the aminoglycoside were determined using RDKit tools (RDKit: Open-source cheminformatics, https://www.rdkit.org, https://doi.org/10.5281/zenodo.7415128) as described by [31].

2.6 | AME sequence comparison

Only peptide chain involved in the binding of aminoglycosides was considered for the comparison of AMEs sequences. Sequences were aligned and compared by using the water EMBOSS package (v.6.6.0.0, EMBL-EBI, Cambridgeshire, United Kingdom). The default settings were used: EMBLOSUM62 as the comparison matrix, a gap opening of 10, and a gap extension set as 0.5. Alignments with a length of less than 100 amino acids were not taken into account.

2.7 | RNA sequence comparison

The identity of the sequences was calculated by the local comparison of a consensus AGA binding site, which comprises G1488 to G1497 on the direct strand and C1404 to C1412 on the reverse strand.

3 | RESULTS

In order to study how aminoglycosides bind to AMEs and bacterial RNA, we retrieved all PDB entries that featured neomycin B or kanamycin A bound to any AME or to the bacterial ribosomal A site. We identified the specific interactions present in each complex and mapped them onto 2D structures of the aminoglycoside as pharmacophoric points. The study begins by examining the various binding modes and conformations of neomycin B, which enable it to bind to different AMEs and to the bacterial ribosomal A site. Then, we repeat these analyses for kanamycin A.

A total of 29 PDB files of aminoglycosides in complex with AMEs were explored, 10 containing neomycin B and 19 containing kanamycin A (Table 1). Several entries in the dataset contained multiple copies of an aminoglycoside-AME complex, resulting in 92 complexes being analyzed in this study. Of these complexes, 22 involved neomycin B and 70 involved kanamycin A. Four PDB entries containing neomycin B were discarded due to covalently linked structures or because of not passing one step of the protocol (PDB ID: 6NMM, 6NMN, 6P08, and 7Q1X). Overall, the structures are of good resolution and exhibit good local precision. According to the twilight classification, in 79 of structures, the model correctly fits the electron density (RSCC > 0.8). Out of the analyzed structures, only 13 had an RSCC coefficient lower than 0.8 or were missing this value altogether. As a result, these structures need to be approached with caution. However, in order to avoid losing valuable information regarding the binding of aminoglycosides to certain AMEs, these structures were still included in the study. Any new insights that may be gained from these structures will be noted and carefully interpreted.

The studied dataset covers the three AME types: AAC, APH and ANT. The AACs and APHs activities have been found in other enzymes. AACs belong to the GCN5-related N-acetyltransferases superfamily whereas APHs function as protein kinases. No enzyme superfamily has been associated with ANTs [15, 32, 33]. In spite of a common function, enzymes in the same class can bear little resemblance at the level of their sequence. In the studied dataset, the highest sequence identity between AMEs binding neomycin B is 23.3% (between APH(3')-IIIa and the phosphotransferase of AAC(6')-Ie/APH(2'')-Ia). Of note crystallographic complexes containing engineered mutated versions of ANT(4')-Ia (T130 K and T130 K/E52D) were included in the study as the arrangement of their active site and catalytic function remained unchanged. However, the doubly mutated enzyme (T130 K/E52D) modifies the binding to metal ions, resulting in a weaker binding to neomycin [34]. The dataset contains more AMEs targeting kanamycin, and not unexpectedly their comparison revealed close homolog pairs. For example, the sequence identity is 60% between the acetyltransferase protomer of AAC(6')-Ie/APH(2'')-Ia and APH(6')-Im. The three APH(3') enzymes share between 30 and 35% identical sequence. In brief, the dataset studied illustrates the diversity of AMEs binding neomycin B or kanamycin A, but also presents versatile enzymes acting on the two aminoglycosides.

TABLE 1 Studied PDB entries containing neomycin B or kanamycin A in complex with an AME or RNA.

Aminoglycoside-modifying enzyme				PDB ID	
Type	Targeted position	Resistance profile	Identifier	Neomycin B	Kanamycin A
AAC	3	III	B	6MB5[1], 6MB9[4]	
		VI	A		6O5U[1]
	2'	I	C		1M4I[2]
			D	7CS1[2]	
	6'	I	e*		4QC6[2]
		I	M		6BFH[1]
APH	3'	I	A		4FEU[6], 4FEV[6], 4FEW[6], 4FEX[5], 4GKH[12], 4GKI[12]
		II	A		1ND4[2]
		III	A	2B0Q[1]	1L8T[1]
	2''	I	a*	5IQE[4]	5IQB[4]
		I/IV	d/a		3SG9[2], 4DFB[2], 4DFU[2]
		III	A		6CTZ[1]
ANT	4'	I	A	6UN8[2]	1KNY[2]
			a/T130K mutant	6NMK[2], 6NML[2]	
			a-T130K/E52D mutant	6P04[2], 6P06[2]	
	2''	I	A		4WQL[1]
RNA	A site			2A04[2], 2ET4[2]	2ESI[2]
	30S ribosomal subunit from *Thermus thermophilus*			4LF6[1], 4LFB[1]	
	70S ribosome from *E. coli*			4V52[2], 4V57[2], 4V9C[2]	

The superscript indicates the number of aminoglycoside copies. *Refers to the bifunctional enzyme AAC(6')-Ie/APH(2'')-Ia.

Regarding RNA complexes, 8 PDB entries were studied, 7 containing neomycin B and 1 kanamycin A (Table 1). These complexes contained a total of 12 neomycin B and 2 kanamycin A bound to site A. All structures had an RSCC >0.8, fitting the electron density. The RNA sequences constituting the studied binding site are identical between five of the PDB entries (PDB ID: 2A04, 2ET4, 4V9C, 4V52, and 4V57) and share 90% identity with the two other sequences (PDB ID: 4LF6 and 4LFB).

Each of the analyzed structures have been prepared using a standardized protocol to obtain an all-atoms description of the AGA-AME/RNA complex. Missing hydrogen atoms have been added and placed at the most probable position based on the construction of an optimal hydrogen bonding network [27]. Based on the hydrogen configuration, hydrogen bonds, ionic bonds, and metallic interactions between AGAs and AMEs/RNA have been detected based on geometrical rules, such as specific distances and angles. Since water molecules can play an important role in stabilizing the complex and mediating interactions between the AME/RNA and the AGA, we considered that water molecules forming two or more hydrogen bonds with the protein were tightly bound to the protein and, therefore, were part of the binding site.

3.1 | Neomycin B in complex with AMEs and RNA

The 22 structures of neomycin B and AME complexes are distributed across five enzyme classes, including two AACs, two APHs and one ANT (Table 1). When considering all classes collectively, it has been observed that each of the four aminoglycoside rings is accommodated by at least two enzyme classes, and nearly all of the nitrogen and oxygen atoms in the aminoglycoside are utilized by at least one of the enzymes (Figure 2A). Additionally, for each enzyme considered individually, a significant portion of the aminoglycoside interacts with the protein site. The total number of polar interactions per complex ranges from 11 with AAC(3)-IIb (PDB ID: 6MB9) to 27 with APH(2'')-Ia (PDB ID: 5IQE) (Figure 2C), including hydrogen bond (HB), ionic bonds and an interaction with a metallic cation. When

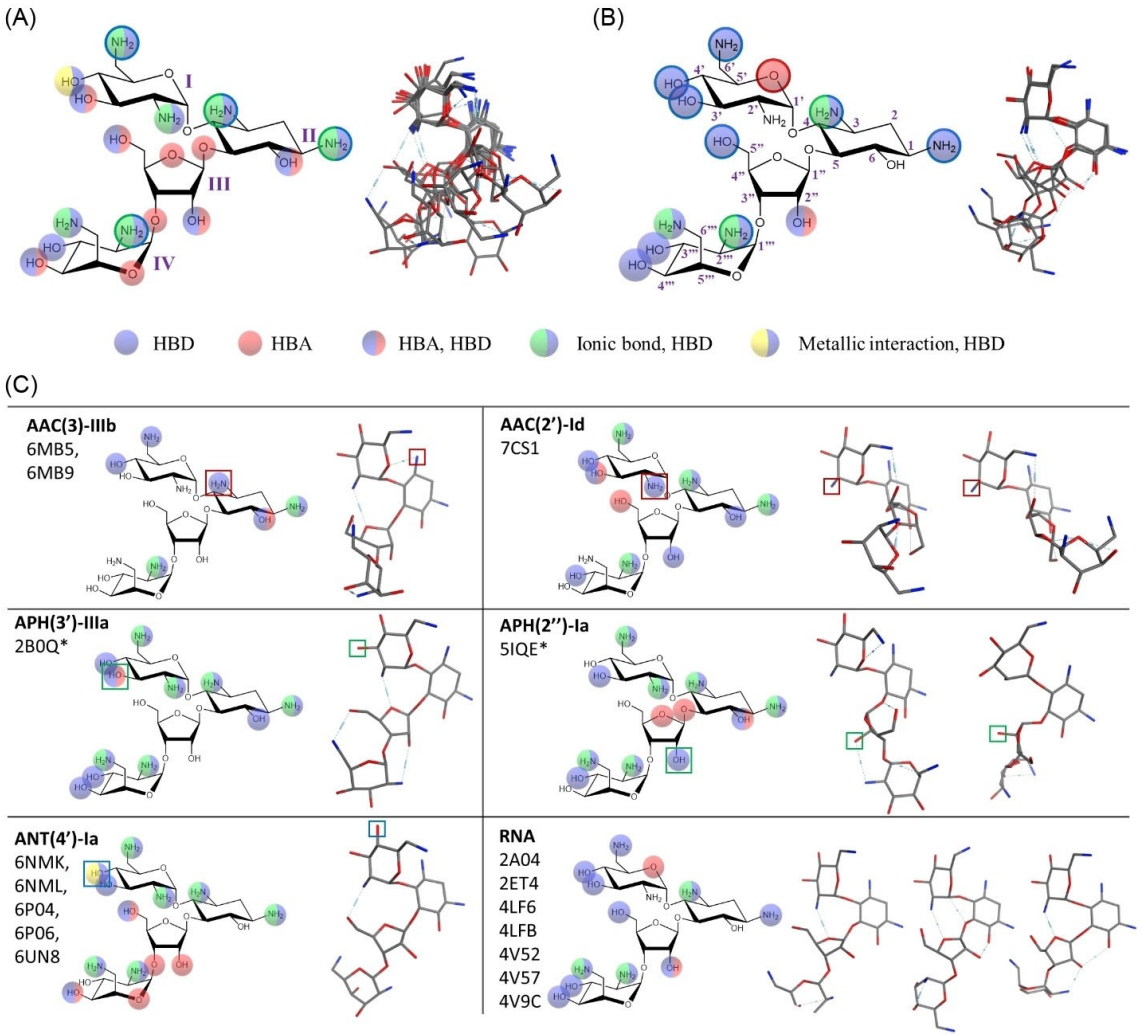

FIGURE 2 2D and 3D representation of neomycin B. (A) ensemble of all neomycin B-AME interactions and neomycin B conformers superposed on rings I and II. Outlined interactions are present in all AMEs. (B) ensemble of all neomycin B-RNA interactions and neomycin B conformers superimposed on rings I and II. Outlined interactions are present in all PDB entries. (C) 2D and 3D structures of neomycin B per AME and RNA. A colored square marks the targeted position. On the right, all neomycin B conformations binding the enzyme are depicted. The symbol * identifies low scored RSCC structures.

examining neomycin B, attention is directed towards its seven hydroxyl groups and six amino groups. Among hydroxyl groups, all are capable of acting as hydrogen bonding donors (HBD), with one group also interacting with a metallic cation. Additionally, five of these hydroxyl groups can also act as hydrogen bonding acceptors (HBA). When considering the amino groups, it is predicted that they will be positively charged in all of the studied complexes except for one of the complexes of ANT(4')-Ia (PDB ID: 6MNK). Furthermore, all six of these groups are involved in salt bridges that are assisted by hydrogen bonding. The other polar atoms of neomycin are oxygen atoms in the ether groups which are present in rings I, III and IV as well as in the three linkages connecting the four rings. Compared to the hydroxyl and amino groups, the ether groups of neomycin B play a minor role in the recognition of the AMEs, as only those located in or near the ring IV are recognized by the ANT(4')-Ia, and those located in or near the ring II are recognized by APH(2'')-Ia. It should be noted that the accessibility of the oxygen atom in ether groups is limited due to steric hindrance.

Water-mediated hydrogen bonds were detected in all investigated PDB files, with a maximal number of 9 and an average number of 3 ± 2, suggesting that water plays a role in the recognition of neomycin B by all types of AMEs. The quantity and arrangement of water molecules are contingent upon the AME, yet are not always consistent. In some PDB files that include multiple copies of the same complex, there may be both structures with and without water-mediated hydrogen bonds (e.g., PDB IDs 6MB9, 5IQE and 6P04). Several water-mediated

hydrogen bonds are by contrast well conserved: with C(1)-NH_2 in four out of the five copies of AAC(3)-IIIb; with C(3)-NH_2, C(4')-OH, and C(6')-NH_2 in the two copies of AAC(2')-Id ; with C(3)-NH_2, C(6')-NH_2, and C(6''')-NH_2 in seven out of ten copies of ANT(4')-Ia; and with C(5'')-OH in 5 of the copies of ANT(4')-Ia.

Noteworthy, the catalytic activities of APH and ANT require a metallic ion, yet the structures show a direct interaction between neomycin B and the metal only in ANT(4')-Ia.

Regarding RNA complexes, neomycin B binds to several binding sites other than the ribosomal A site on the structures showing the 30S ribosomal subunit. Here, we focus on the bacterial ribosomal A site binding. In all but one of the studied complexes (PDB ID: 4V9C), all six amino groups of the aminoglycoside are positively charged. Neomycin B uses three hydroxyl groups, four amino groups, and one ether to bind the ribosomal A site in all 12 structures (Figure 2B, see outlined interactions). Rings I and II form six out of the eight interaction which are conserved across the studied complexes, while rings III and IV show a binding mode dependent on the PDB structure. Interestingly, C(6')-NH_2 and with C(1)-NH_2 do not form ionic bonds contrarily to the interactions with the AMEs. Also, C(2')-NH_2 and C(6)-OH do not interact with the RNA while they appear to be part of the binding mode for five out of four AME complexes. Among all polar groups of neomycin B, C(3)-NH_2 is the one which forms the higher number of interactions, including hydrogen and ionic bonds with two nucleotides (A1493 and G1494).

Only two water mediated interactions have been detected among the structures of the RNA complexes: one interacting with C(6')-NH_2 and a second one interacting with C(5'')-OH.

The comparison of the binding modes of neomycin B to the different protein classes points out the singularity of AACs (Figure 2C). All studied enzymes interact with most of the aminoglycoside polar groups, while AAC(3)-IIIb only forms six polar interactions, including five with rings I and II. Additionally, the other AAC of the dataset, namely AAC(2')-Id, also form fewer interactions with ring IV than the APHs and ANTs. Given that rings I and II participate in numerous interactions between neomycin and its protein binding site, irrespective of the enzyme type, we assessed whether this substructure of the aminoglycoside exhibits conformational diversity or instead adopts a consistent conformation across various AMEs.

Figure 2A shows the superimposition of the 22 structures of neomycin B, after their 3D alignment for the best overlay of rings I and II. The conformation of rings I and II, i.e. neamine, is pretty conserved across the five AMEs. However, Figure 2C shows that neomycin B adopts two different conformations when binding AAC(2')-Id and APH(2'')-Ia. The distribution of the torsion angles of the linkages between the rings presented in Figure 3 more finely characterizes the conformational variations of the AME-bound forms of neomycin B. The linkage between rings I and II show conserved phi and psi angles, although the clustering of the values segregates the AMEs by type. While dihedral angles forming the bonds linking rings I and II move on a range of approximately 60°, bonds linking rings II–III and III–IV can differ by 180° providing a total new conformer. Despite a few exceptions, it is also noticeable that the dihedral angles are grouped by type of AME and so, that neomycin B's conformations are adapted to the environment. The biggest difference is shown by the structure represented in AAC(2')-Id (PDB code: 7CS1),

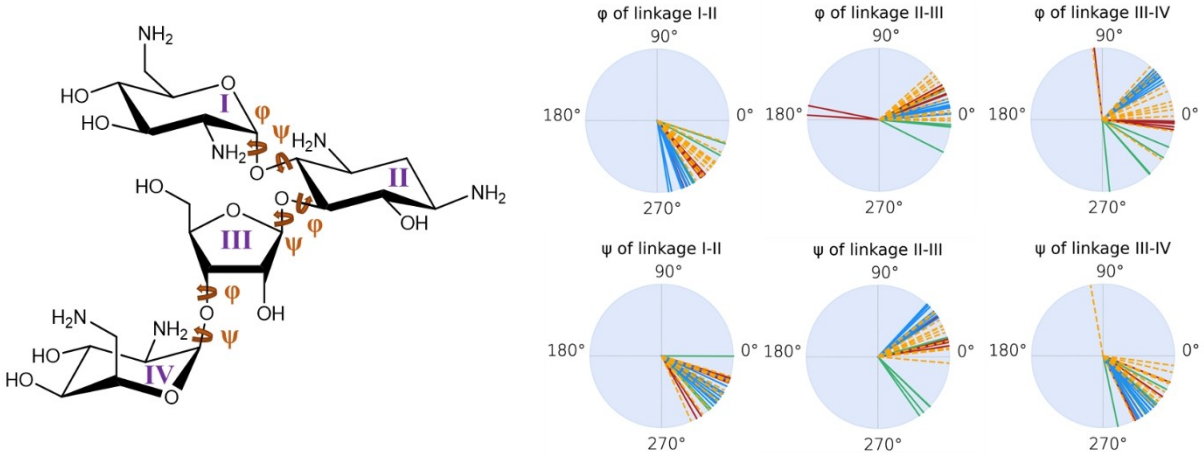

FIGURE 3 Comparison of neomycin B conformers dihedral angles. Red color is attributed to conformers bound to AAC, green to APH, blue to ANT, and dashed orange to RNA. Atoms forming dihedral angles were defined following Ref. [37]: ϕ(H1-C1-O1-Cx) and ψ(C1-O1-Cx-Hx).

where the ϕ angle of the bond linking ring II to III has rotated 180° compared to the other structures. The same thing happens for the ϕ angle of the linkage between rings III and IV of one of the two conformers of the enzyme. This mobility of rings III and IV can be appreciated in Figure 2A. Actually, the left conformation of AAC(2')-Id forms all the interactions shown on the 2D structure except the hydrogen bond with C(4')-OH on ring I, while the right conformation loses almost all the interactions formed by rings III and IV, only keeping the bridge salt formed by C(2''')-NH_2 of ring IV. APH(2'')-Ia (PDB code: 5IQE) also presents two conformers. The right structure, being the structure having a low RSCC, differentiates itself by adding up the hydrogen bond interaction formed by the C(3''')-OH of ring IV and the acceptor feature of the hydrogen bond formed by C(6)-OH of ring II. Neomycin B conformers binding APH(2'')-Ia are the ones showing the biggest difference of ψ angle for linkage II–III and of ϕ angle of rings III and IV on Figure 3.

Neomycin B bound to the bacterial ribosomal A site also has a conserved neamine conformation in all complexes, while rings III and IV have a higher mobility. Interestingly, the conformations it adopts are similar to those adopted when in complex with AMEs (Figure 3). In one of the neomycin B – RNA structures (PDB code: 4V9C), ring IV is rotated of 180° (Figures 2A, B and 3) similarly to the unique ϕ angle of the linkage between rings III and IV present in AAC(2')-Id.

In conclusion of the structural analysis, the binding of neomycin B to AME complexes is primarily governed by polar interactions, which is consistent with the highly polar and positively charged characteristics of the aminoglycoside and the complementary properties of the protein binding sites. This conclusion is supported by 448 polar interactions and hydrophobic contacts presented in Figure 3A, where 69% of data involve glutamic and aspartic acids, i.e. negatively charged residues in AMEs. Additionally, water molecules significantly contribute to the binding, accounting for 14% of the interactions. Finally, neomycin B acquires its flexibility from the bonds linking rings II to III and III to IV, keeping a conserved neamine conformation in all complexes. The binding mode and conformations of neomycin B when bound to RNA and AME are similar. However, ionic bonds are less common in RNA complexes and HBA are practically excluded from the binding mode.

3.2 | Kanamycin A in complex with AMEs and RNA

Figure 4 collects all interactions with AMEs and conformations that kanamycin A presents in 70 structures (Table 1). As for neomycin B, all rings and polar groups of kanamycin A are involved in the binding to AMEs, and the bonding is dominated by polar interactions (Figure 2). The number of interactions formed by kanamycin A ranges from 8 to 26, with 20 being the average.

All seven kanamycin hydroxylic groups are able to adjust their role of HBD or HBA to the enzyme. One of them also involves a metallic interaction. Amino groups are essential to form ionic bonds with the AMEs. In fact, of a total of 1489 interactions when combining all structures, 885 of them occur with aspartic acid and glutamic acid. Apart from ionic bonds, all four amino functions also act as HBD. In the case of kanamycin A, only two over four ether functions act as HBA.

As mentioned, all three rings interact in all AME-kanamycin A structures. However, ANT(2'')-Ia is the only AME forming just three ionic bonds with three amino groups and a metallic interaction. All the other complexes involve a minimum of two hydrogen bonds formed by the hydroxylic groups and do not have any metallic interaction. AAC(2')-Ic is included in the analysis even though kanamycin A cannot be metabolized by the AME as the targeted position is a hydroxyl group instead of an amino group (Figure 1).

The water network is also important for the binding of kanamycin A as it is responsible for at least one interaction in 61 of the 70 structures. In average, it is responsible for 4 ± 2.5 interactions per complex, and for some complexes water forms up to 7 hydrogen bonds with the aminoglycoside. ANT(4')-Ia and ANT(2'')-Ia are the only two AMEs not implicating any water molecules on the binding mode. Several water-mediated hydrogen bonds are well conserved among the other complexes: with C(3)-NH_2 for all copies of AAC(2')Ic, AAC(3)-VIa, and APH(3')-IIa, 38 copies out of 47 of APH(3')-Ia, and one copy out of two of AAC(6')- Ie; with C(6')-NH_2 for all copies of AAC(6')Im, AAC(2')-Ic, AAC(3)-VIa, and APH(2'')-Ia, and 23 copies out of 47 of APH(3')-Ia one copy out of two of AAC(6')-Ie and APH(3')-IIa; with C(2')-OH for all copies of APH(3')-IIIa, APH(2'')-IIIa, 32 copies out of 47 of APH(3')-Ia, and one copy of AAC(2')-Ic and APH(3')-IIa; and finally with the O linking rings I and II in all copies of APH(3')-IIa, APH(3')-IIIa and 30 out of 47 of APH(3')-Ia.

Kanamycin A binds to RNA by using all four amino groups and four out of seven hydroxyl groups (Figure 4B). Kanamycin A binding is mainly led by seven HBD interactions and two ionic bonds formed by

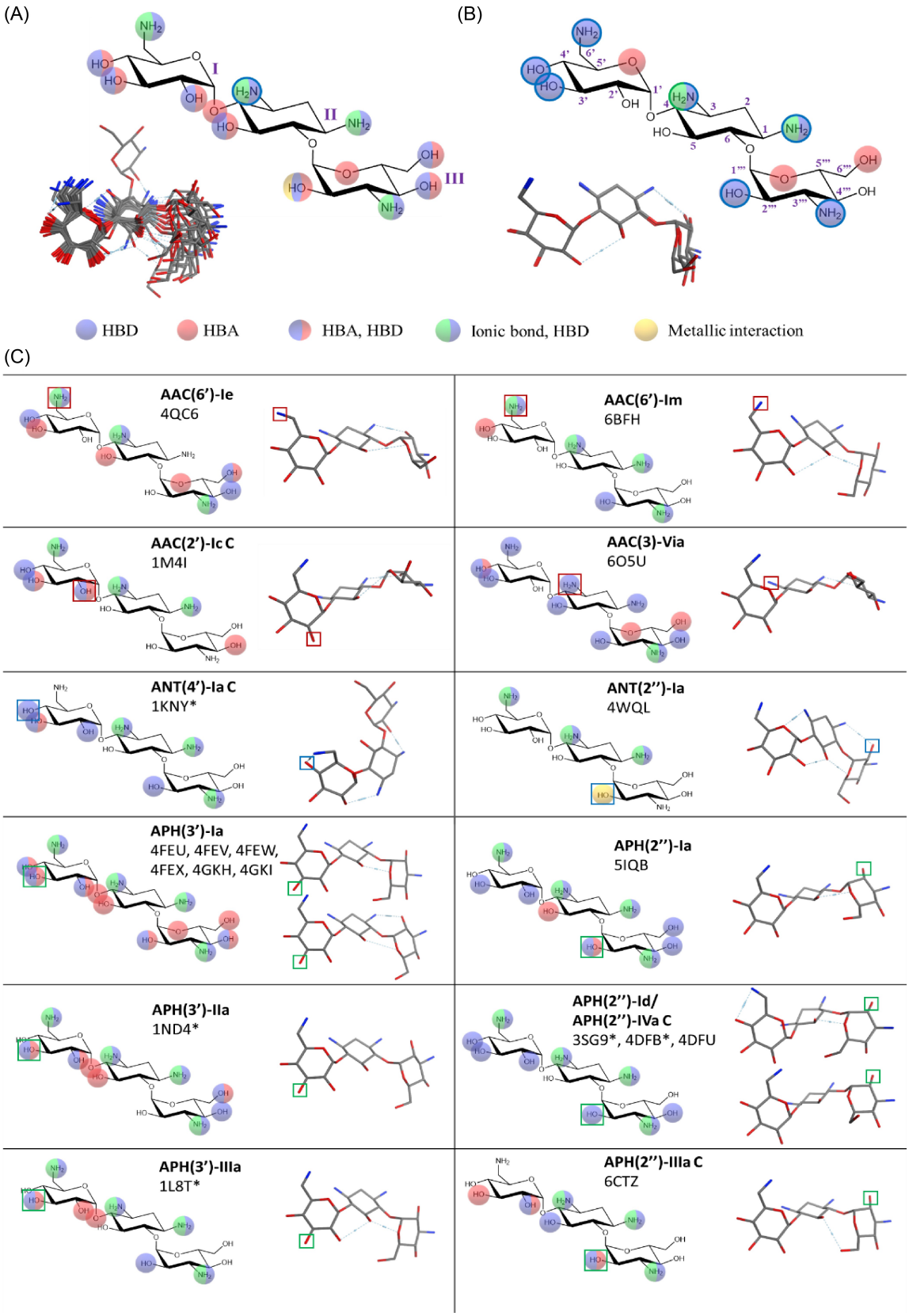

FIGURE 4 2D and 3D representation of kanamycin A RX-structures. (A) ensemble of all kanamycin A-AME interactions and kanamycin A conformers superimposed on rings I and II. Outlined interactions are present in all AMEs. (B) ensemble of all kanamycin A-RNA interactions and kanamycin A conformers superimposed on rings I and II. Outlined interactions are present in both RNA complexes. (C) 2D and 3D structures of kanamycin A per AME. A colored square marks the targeted position. On the right, all kanamycin A conformations binding the enzyme are depicted. The symbol * identifies low scored RSCC structures.

C(3)-NH_2 as shown by the outlined interactions in Figure 4B. In the case of kanamycin A, the three rings are implicated in the binding mode.

The superimposition of kanamycin A conformers (Figure 4A) shows a smaller conformational variability of this aminoglycoside as compared to neomycin B. All conformers except one are spatially very close to each other. The RMSD study, assigning new clusters if the RMSD difference is higher than 0.5 Å, revealed only 2 clusters of conformers. Only the aminoglycoside binding ANT(4')-Ia totally differs from all other structures. All three ψ of linkage I–II, ϕ and ψ of linkage II–III dihedral angles are inversed when compared to the other conformers. On another side, both linkages seem equally responsible for flexibility, but the ϕ angle of linkage II–III seems to differentiate the kanamycin A binding APH, with angles between 24° and 67°, from those binding AAC, with angles ranging from 348° to 357° if we ignore AAC(6')-Im with an angle of 22° (Figure 5). This angle difference can be observed in Figures 4A and C.

If we exclude the previously discussed exceptions, kanamycin A conformers bound to AME have similar dihedral angles to those bound to site A.

As with neomycin B, kanamycin A – AME complexes are governed by polar interactions. More than half of the interactions (59%) involve either glutamic acid or aspartic acid. The water network is again very important, acting as a bridge in 19% of interactions. Finally, the conformers of bound kanamycin A defined only two clusters even though the torsion angle ranges showed variations.

4 | DISCUSSION

AMEs constitute the principal mechanism of bacterial resistance to AGAs. Our study provides structural insights into two AGAs, neomycin B and kanamycin A, which are representative of four- and three-rings structures, respectively. We systematically analyzed the conformation and binding mode of the AGAs in AMEs, and for the sake of comparison to the target site in RNA. All available data was extracted from the PDB, protonated and standardized. A total of 37 files were explored, corresponding to the 116 crystallographic structures of AGA. The studied dataset covers the three AME types (AAC, APH, and ANT) and bacterial rRNA. The structural analysis involved the identification of non-covalent interactions, their mapping onto 2D structures, the assessment of the importance of water-mediated interactions, and the characterization of AGAs conformations.

Our analysis demonstrated that the recognition of both neomycin B and kanamycin A is primary driven by multiple polar interaction, predominantly hydrogen bonds. Water-mediated hydrogen bonds play a significant role, consistently comprising 14–19% of the polar interactions. Our study also revealed that both neomycin B and kanamycin A tend to form more ionic interactions with the AMEs compared to RNA.

AMEs in the dataset, although sharing common functional features, have different sequences and exhibit unique active sites. Consequently, AGAs adopt distinct binding modes and conformations in different AMEs. Nevertheless, there is trend common to all studied AGA-AME complexes: the neamine moiety, made of ring I

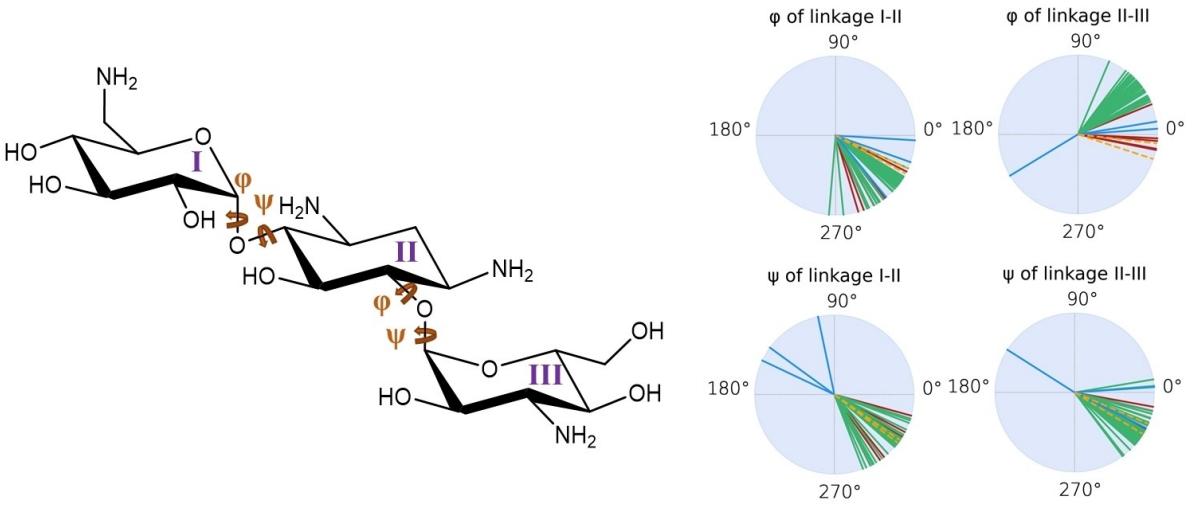

FIGURE 5 Comparison of kanamycin A conformers dihedral angles. Red color is attributed to conformers bound to AAC, green to APH, blue to ANT, and dashed orange to RNA. Atoms forming dihedral angles were defined following Ref. [37]: ϕ(H1-C1-O1-Cx) and ψ(C1-O1-Cx-Hx).

and II, shows a well-conserved conformation across all of the structures.

The ability of neomycin B and kanamycin A to adapt to different protein environments of APH(3')-IIIa and ANT(4')-Ia is illustrated in Figure 6. Interestingly, the two aminoglycosides show similar binding mode to APH(3')-IIIa (Figure 6A and B), involving the same amino acids to bind the neamine moiety. Thus the AGA target position in ring I is well aligned with the active site. The rings III and IV of neomycin B occupy a larger portion of the enzyme's catalytic pocket than ring III of kanamycin A, and as a result form a greater number of interactions with the enzyme. By contrast, neomycin B and kanamycin A bind completely differently to the wide active site of ANT(4′)-Ia, the only common feature being the location of AGA target position (Figures 6C and D).

Overall, the comprehensive study of the PDB emphasized the diversity of binding modes, highlighting the versatility of both the AMEs and AGAs.

4.1 | How to escape AMEs: the amikacin example

Amikacin is a semisynthetic derivative of kanamycin A introduced in the seventies. It is substituted at the position C(1)-NH_2 by a (S)-4-amino-2-hydroxybutyrate (HABA) (Figure 7A). Like the other aminoglycosides, it is active against Gram+ and Gram- bacteria, and, together with plazomicin, amikacin demonstrates higher resistance to the action of AMEs. Nevertheless, there has been an emergence of resistant strains, particularly associated with the rise of AAC(6')-Ib, limiting its effectiveness [35].

The analysis of amikacin intends to provide insights into the potential of designing new AGAs derivatives based on the crystallographic structures. Amikacin has been described in four crystallographic structures: two in complex with rRNA (PDB ID: 4P20 and 6YPU), one in complex with APH(2'')-Ia, GMPPNP, and Mg^{2+} (PDB ID: 6CGD), and one in complex with AAC(2')-Ia and AcCoA (PDB ID: 6VTA).

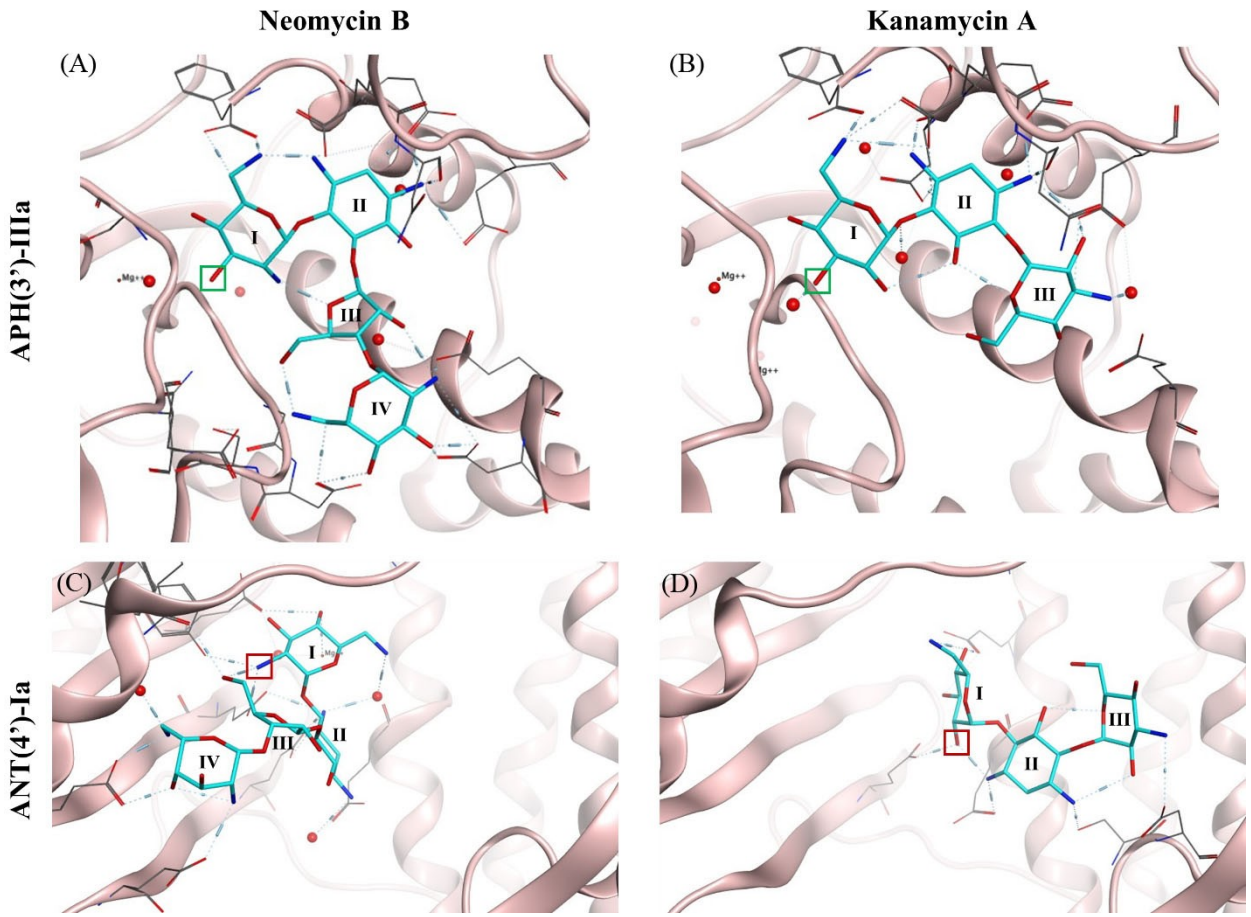

FIGURE 6 Comparison of the binding modes of (A) neomycin B/APH(3')-IIIa (PDB ID: 2B0Q), (B) kanamycin A/APH(3')-IIIa (PDB ID: 1L8T), (C) neomycin B/ANT(4')-Ia (PDB ID: 6UN8), and (D) kanamycin A/ANT(4')-Ia (PDB ID: 1KNY). Only the interacting residues are depicted. A colored square marks the targeted position. Water molecules are depicted as red spheres.

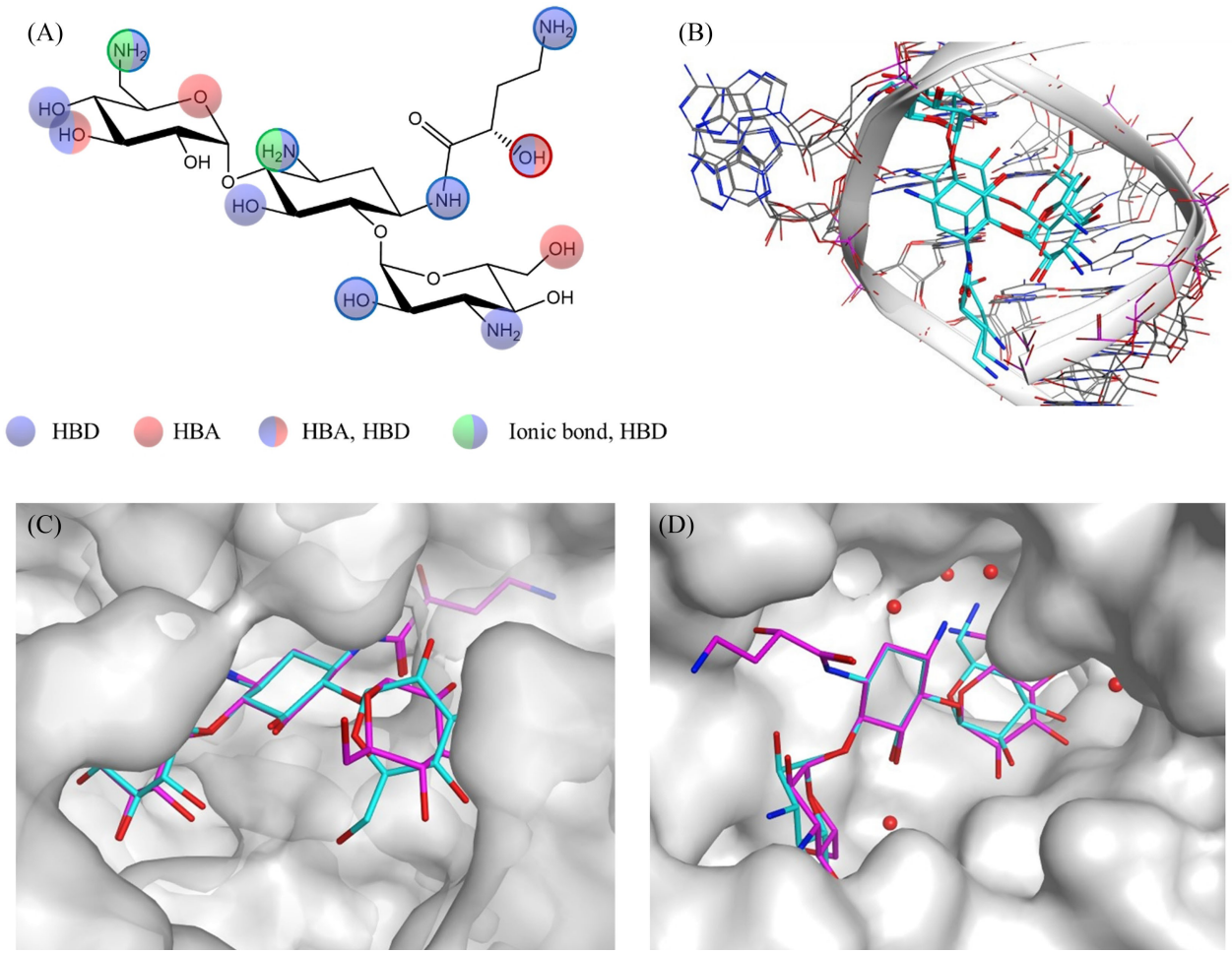

FIGURE 7 2D and 3D representation of amikacin. (A) Ensemble of all amikacin-RNA interactions. Outlined interactions are present in all in RX-structures in of amikacin in complex with rRNA (B) superimposed amikacin-RNA 3D structures. (C) Superimposition of amikacin (pink) onto kanamycin A (blue) ring II bound to APH(3')-IIIa. (D) Superimposition of amikacin (pink) onto kanamycin A (blue) ring II bound to AAC(6')-Ie.

In complex with rRNA, amikacin engages its three rings in polar interactions, including hydrogen bonds with all five amino groups and five out of seven hydroxyl groups, and ionic bonds for two amino groups (Figure 7A). Furthermore, all amikacin conformers adopt a conformation similar to that of kanamycin A when bound to rRNA (Figures 7B and 5), suggesting that the HABA substitution does not interfere with the AGA recognition by the target in the bacterial ribosome. The C(1)-NH_2 of both amikacin and kanamycin A is able to form a stable hydrogen bond with U1492. In addition, the HABA chain also form polar interactions with rRNA (Figure 7A, B). The superimposition of a crystallographic structure of amikacin onto kanamycin A bound to APH(3')-IIIa (Figure 7C) suggested steric hindrance in the presence the HABA chain. Indeed, the C(1)-NH_2 was involved in the binding mode of all complexes AME/kanamycin A, except for AAC(6')-Ie. Interestingly, the main amikacin resistance mechanisms are AAC(6')-I enzymes and in particular AAC(6')-Ib [35]. The structure of the amikacin bound to AAC(6')-Ie modeled from the kanamycin A complex indicated that the HABA chain would not disrupt recognition of the enzyme.

In summary, the comparison of kanamycin A and amikacin demonstrated that structural considerations can offer strong evidence to predict the impact of a chemical modification of the AGA on its binding to both RNA and AMEs.

5 | CONCLUSION AND PERSPECTIVES

Designing new aminoglycosides able to overcome AMEs effect has been a challenging and long-standing task. While derivatives of kanamycin A, such as amikacin, have been identified in this pursuit, the antimicrobial resistance landscape continues to increase. The

comprehensive analysis of crystallographic structures containing neomycin B and kanamycin A, two common aminoglycosides, revealed the versatility of the two AGAs which exhibit multiple binding modes within different enzyme environments. This adaptability significantly complicates the task of finding a common modification that can overcome the resistance caused by all AMEs simultaneously. The intricacy of the problem is heightened by the promiscuity of AMEs, whose adaptability exploits various molecular properties, encompassing active site breadth for ANT, local flexibility for AAC, and multiple conformations for APH [36].

The detailed interactions formed by AGAs provides avenue to guide the design of new derivatives capable of overcoming AMEs. The focus can be set on disrupting crucial hydrogen bonds for recognition, modulating water-mediated interactions, disrupting ionic interactions as they mainly interact with AMEs, and introducing steric hindrance.

AUTHOR CONTRIBUTIONS

JRI and EK designed the project. JMW, EE, and GP contributed to validating the study sample. JRI implemented the approach, performed the experiments and analyzed the data. EK supervised the project. JRI and EK drafted the manuscript. All authors contributed to the refinement of the manuscript.

ACKNOWLEDGEMENTS

The authors acknowledge the High-Performance Computing Center of the French National Institute for Nuclear and Particle Physics (IN2P3). This work was supported by Centre National de la Recherche Scientifique (CNRS) and Université de Strasbourg (IDEX consolidation W19RHUS3). This work of the Interdisciplinary Thematic Institute IMS, the drug discovery and development institute, as part of the ITI 2021–2028 program of the University of Strasbourg, CNRS and Inserm, was supported by IdEx Unistra (ANR-10-IDEX-0002), and by SFRI-STRAT'US project (ANR-20-SFRI-0012) under the framework of the French Investments for the Future Program.

DATA AVAILABILITY STATEMENT

The prepared structure files are accessible via an online repository (https://seafile.unistra.fr/d/1929bd159acf418d8906/).

ORCID

Esther Kellenberger http://orcid.org/0000-0002-9320-4840

REFERENCES

1. M. L. Avent, B. A. Rogers, A. C. Cheng, D. L. Paterson, *Intern. Med. J.* **2011**, *41*, 441–449.
2. K. M. Krause, A. W. Serio, T. R. Kane, L. E. Connolly, *Cold Spring Harb. Perspect. Med.* **2016**, *6*, a027029.
3. J. Davies, L. Gorini, B. D. Davis, *Mol. Pharmacol.* **1965**, *1*, 93–106.
4. D. Moazed, H. F. Noller, *Nature* **1987**, *327*, 389–394.
5. J. L. Houghton, K. D. Green, W. Chen, S. Garneau-Tsodikova, *ChemBioChem* **2010**, *11*, 880–902.
6. U. S. Gonzalez, J. P. Spencer, *Am. Fam. Physician* **1998**, *58*, 1811–1820.
7. M.-P. Mingeot-Leclercq, P. M. Tulkens, *Antimicrob. Agents Chemother.* **1999**, *43*, 1003–1012.
8. T. Hutchin, I. Haworth, K. Higashi, N. Fischel-Ghodsian, M. Stoneking, N. Saha, C. Arnos, G. Cortopassi, *Nucleic Acids Res.* **1993**, *21*, 4174–4179.
9. E. C. Böttger, D. Crich, *ACS Infect. Dis.* **2020**, *6*, 168–172.
10. *WHO Model Lists of Essential Medicines.* https://www.who.int/groups/expert-committee-on-selection-and-use-of-essential-medicines/essential-medicines-lists
11. M. Galimand, S. Sabtcheva, P. Courvalin, T. Lambert, *Antimicrob. Agents Chemother.* **2005**, *49*, 2949–2953.
12. Y. Doi, J.-I. Wachino, Y. Arakawa, *Infect. Dis. Clin. North Am.* **2016**, *30*, 523–537.
13. K. Poole, *Ann. Med.* **2007**, *39*, 162–176.
14. R. E. W. Hancock, *J. Antimicrob. Chemother.* **1981**, *8*, 249–276.
15. M. S. Ramirez, M. E. Tolmasky, *Drug Resist. Updat. Rev. Comment. Antimicrob. Anticancer Chemother.* **2010**, *13*, 151–171.
16. N. T. Chandrika, S. Garneau-Tsodikova, *Chem. Soc. Rev.* **2018**, *47*, 1189–1249.
17. A. N. Tevyashova, K. S. Shapovalova, *Pharm. Chem. J.* **2021**, *55*, 860–875.
18. J. Obszynski, H. Loidon, A. Blanc, J.-M. Weibel, P. Pale, *Bioorganic Chem.* **2022**, *126*, 105824.
19. K. M. Shaeer, M. T. Zmarlicka, E. B. Chahine, N. Piccicacco, J. C. Cho, *Pharmacother. J. Hum. Pharmacol. Drug Ther.* **2019**, *39*, 77–93.
20. T. Golkar, A. V. Bassenden, K. Maiti, D. P. Arya, T. M. Schmeing, A. M. Berghuis, *Commun. Biol.* **2021**, *4*, 1–8.
21. Q. Vicens, E. Westhof, *Biopolymers* **2003**, *70*, 42–57.
22. A. P. Carter, W. M. Clemons, D. E. Brodersen, R. J. Morgan-Warren, B. T. Wimberly, V. Ramakrishnan, *Nature* **2000**, *407*, 340–348.
23. M. A. Cook, G. D. Wright, *Sci. Transl. Med.* **2022**, *14*, eabo7793.
24. *RCSB PDB: Homepage.* https://www.rcsb.org/(accessed: 2022–04-01)
25. E. Kellenberger, P. Muller, C. Schalon, G. Bret, N. Foata, D. Rognan, *J. Chem. Inf. Model.* **2006**, *46*, 717–727.
26. J. Desaphy, G. Bret, D. Rognan, E. Kellenberger, *Nucleic Acids Res.* **2015**, *43*, D399–D404.
27. S. Bietz, S. Urbaczek, B. Schulz, M. Rarey, *J. Cheminformatics* **2014**, *6*, 12.
28. J. Desaphy, E. Raimbaud, P. Ducrot, D. Rognan, *J. Chem. Inf. Model.* **2013**, *53*, 623–637.
29. F. Da Silva, J. Desaphy, D. Rognan, *ChemMedChem* **2018**, *13*, 507–510.
30. F. Pedregosa, G. Varoquaux, A. Gramfort, V. Michel, B. Thirion, O. Grisel, M. Blondel, P. Prettenhofer, R. Weiss, V.

Dubourg, J. Vanderplas, A. Passos, D. Cournapeau, M. Brucher, M. Perrot, É. Duchesnay, *J. Mach. Learn. Res.* **2011**, *12*, 2825–2830.
31. F. Corzana, I. Cuesta, F. Freire, J. Revuelta, M. Torrado, A. Bastida, J. Jiménez-Barbero, J. L. Asensio, *J. Am. Chem. Soc.* **2007**, *129*, 2849–2865.
32. D. M. Daigle, G. A. McKay, P. R. Thompson, G. D. Wright, *Chem. Biol.* **1999**, *6*, 11–18.
33. M. W. Vetting, L. P. S. de Carvalho, M. Yu, S. S. Hegde, S. Magnet, S. L. Roderick, J. S. Blanchard, *Arch. Biochem. Biophys.* **2005**, *433*, 212–226.
34. B. Selvaraj, S. Kocaman, M. Trifas, E. H. Serpersu, M. J. Cuneo, *ACS Catal.* **2020**, *10*, 3548–3555.
35. M. S. Ramirez, M. E. Tolmasky, *Molecules* **2017**, *22*, 2267.
36. J. Romanowska, N. Reuter, J. Trylska, *Proteins Struct. Funct. Bioinforma.* **2013**, *81*, 63–80.
37. F. Corzana, I. Cuesta, F. Freire, J. Revuelta, M. Torrado, A. Bastida, J. Jiménez-Barbero, J. Luis Asensio, *Journal of the American Chemical Society* **2007**, *129*(10), 2849–2865.

How to cite this article: J. Revillo Imbernon, J.-M. Weibel, E. Ennifar, G. Prévost, E. Kellenberger, *Molecular Informatics* **2024**, *43*, e202300339.
https://doi.org/10.1002/minf.202300339

Graphical Abstract

The contents of this page will be used as part of the graphical abstract of html only.
It will not be published as part of main.